"Shadow" model for sub-barrier fusion applied to light systems: Determination of the reaction rate

A. Scalia and P. Figuera
Dipartimento di Fisica Università di Catania and Istituto Nazionale di Fisica Nucleare, Catania I95129, Italy
(Received 4 August 1992)

The fusion cross section is obtained in the framework of the "shadow" model. The parameters, which appear in the analytical expression of the fusion cross section, are determined by fitting the experimental values of the fusion cross section. The cross section factor $\langle \sigma v \rangle$ is obtained by using this fusion cross section and by assuming that the distribution of the relative velocity between two different sets of particles is described by a Maxwell-Boltzmann distribution. The values of $\langle \sigma v \rangle$ at different temperatures are determined by performing numerical integrations. At energies at which the experimental data are available the obtained cross section factor values coincide with those reported in the literature; at very low energies experimental data are not available and our approach is able to give the values of the cross section factor.

PACS number(s): 25.70.Jj, 95.30.Cq

I. INTRODUCTION

The understanding of our cosmic heritage combines astrophysics and nuclear physics and forms what is called nuclear astrophysics. Nuclear fusion plays a key role in nuclear astrophysics. In fact, for the energy production rate in stars or for the course of nucleosynthesis, it is the fusion cross section that is needed. The determination of the nuclear fusion cross section for stellar nucleosynthesis usually requires determining the fusion cross section at as low an energy as feasible; these astrophysical energies are so low, with respect to the Coulomb barrier, that direct measurements are in general impossible, so that the fusion cross section must be extrapolated to still lower energies. A possible approach to determine the fusion cross sections at low energy consists in parametrizing the available experimental data and extrapolating them to lower energies. This method has several drawbacks. In many cases experimental data do not exist. Moreover, the extrapolation is sensitive to the accuracy of the available data, and finally some effects can be hidden in the energy range considered experimentally. In any case this extrapolating procedure is a crucial point for the determination of the reaction rate in nuclear astrophysics. Moreover, the values of the nuclear cross sections adopted in the calculations of the reaction rates are relevant to obtain the neutrino fluxes by using stellar evolutionary codes so that the determination of the "right" expression for the fusion cross section can be considered the "nuclear physics solution" of the solar neutrino problem.

In previous works [1–5], we suggested to determine the reaction rate by using for the fusion cross section the expression obtained in the elastic model or in its generalization (extended elastic models I, II, and III) [1–7]. In the present paper, a systematic analysis of sub-barrier fusion for light systems is performed in the framework of the "shadow" model. We remind the reader that in the shadow model the analytical expression of the fusion cross section is obtained by assuming that the fusion process is the shadow of the elastic scattering [8,9]. To ob-

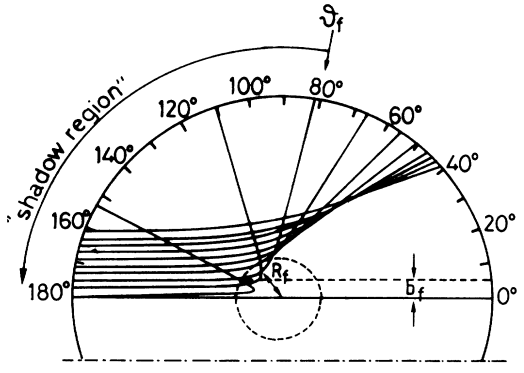

FIG. 1. Rutherford trajectories for different values of the impact parameter. The dashed line shows the range of the strong interaction.

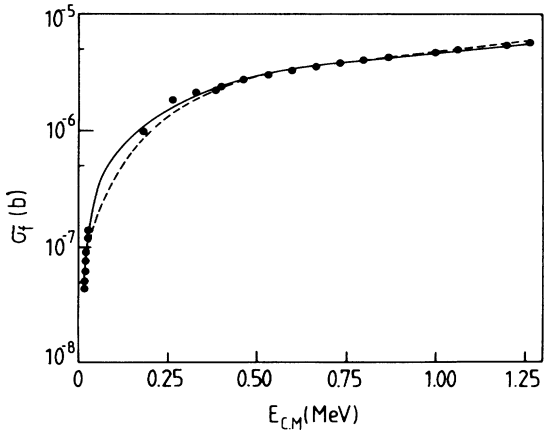

FIG. 2. Comparison for the reaction $^2H(p,\gamma)^3He$ between the experimental values of the fusion cross section [12–14] and the values of σ_f defined in Eq. (8) obtained by using four free parameters (dashed line) and six free parameters (solid line).

TABLE I. Values of the parameters E_B, E_S, y_m, y_1, γ_1, and γ_2 obtained by fitting the experimental data with Eq. (8) using four free parameters (*) and six free parameters (**).

Reactions		E_B	E_S	y_m	y_1	γ_1	γ_2
$^2H(p,\gamma)^3He$	(*)	7.119	7.555	0.8635	0.7517	2.531	0.4496
	(**)	7.671	8.180	0.8518	0.9272	2.421	1.4643
$^2H(d,p)^3H$, $^2H(d,n)^3He$	(*)	0.1809	0.1980	0.8236	0.7057	4.524	2.062
	(**)	0.1892	0.2125	0.8459	0.7181	4.481	3.649
$^3He(d,p)^4He$	(*)	0.1885	0.1650	1.111	1.037	3.870	9.521
	(**)	0.1478	0.1278	1.156	1.003	−0.2297	7.403
$^3He(^3He,2p)^4He$	(*)	1.292	1.269	0.9620	0.8657	5.206	6.808
	(**)	1.337	1.367	0.9179	0.7662	6.439	5.339
$^3He(\alpha,\gamma)^7Be$	(*)	10.51	9.883	1.018	0.9312	4.582	1.504
	(**)	11.84	11.20	1.032	0.9901	3.636	3.760
$^7Li(p,\alpha)^4He$	(*)	1.701	1.913	0.7887	0.6657	3.979	1.787
	(**)	1.797	2.066	0.8158	0.6928	3.786	3.246
$^7Be(p,\gamma)^8B$	(**)	14.5330	13.7724	1.0278	0.9796	2.9478	2.4049

tain the cross-section factor, we determine the parameters which appear in the fusion cross section by fitting the experimental data. After, by assuming that the interacting nuclei collide with a Maxwell-Boltzmann distribution of relative velocity and by using the expression of the fusion cross section obtained in the framework of the shadow model, we obtain the cross-section factor by performing a numerical integration. An extrapolation to low temperature is obtained for the cross-section factor. New numerical procedures are used for systems previous-

TABLE II. Comparison between the values of $N_A\langle\sigma v\rangle$ ($cm^3\,s^{-1}\,mol^{-1}$) obtained with our approach and those reported in Ref. [11] for different systems and at different temperatures corresponding to an energy range where experimental values of fusion cross sections are available.

Reaction	Temperature (K)	$N_A\langle\sigma v\rangle$ Present work	$N_A\langle\sigma v\rangle$ Ref. [11]
$^2H(p,\gamma)^3He$	1.0×10^8	0.663×10^1	0.703×10^1
	3.0×10^8	0.522×10^2	0.653×10^2
	5.0×10^8	0.118×10^3	0.149×10^3
	1.0×10^9	0.338×10^3	0.388×10^3
	3.5×10^9	0.197×10^4	0.153×10^4
$^2H(d,p)^3H$, $^2H(d,n)^3He$	5.0×10^6	0.525×10^0	0.473×10^0
	1.5×10^7	0.473×10^3	0.456×10^3
	2.5×10^7	0.476×10^4	0.496×10^4
	5.0×10^7	0.611×10^5	0.660×10^5
	1.0×10^8	0.461×10^6	0.485×10^6
	1.5×10^8	0.118×10^7	0.125×10^7
	3.0×10^8	0.455×10^7	0.473×10^7
$^3He(d,p)^4He$	3.0×10^7	0.536×10^2	0.586×10^2
	5.0×10^7	0.129×10^4	0.151×10^4
	1.0×10^8	0.590×10^5	0.506×10^5
	3.0×10^8	0.503×10^7	0.447×10^7
$^3He(^3He,2p)^4He$	2.0×10^8	0.870×10^2	0.126×10^3
	3.0×10^8	0.105×10^4	0.134×10^4
	5.0×10^8	0.151×10^5	0.163×10^5
	1.0×10^9	0.219×10^6	0.233×10^6
	2.0×10^9	0.160×10^7	0.170×10^7
$^3He(\alpha,\gamma)^7Be$	3.0×10^8	0.329×10^{-1}	0.555×10^{-1}
	5.0×10^8	0.434×10^0	0.757×10^0
	1.0×10^9	0.688×10^1	0.122×10^2
	2.0×10^9	0.544×10^2	0.924×10^2
	3.5×10^9	0.219×10^3	0.297×10^3
$^7Li(p,\alpha)^4He$	1.0×10^8	0.446×10^2	0.477×10^2
	3.0×10^8	0.677×10^4	0.660×10^4
	5.0×10^8	0.368×10^5	0.362×10^5
	1.0×10^9	0.229×10^6	0.237×10^6
	2.0×10^9	0.924×10^6	0.934×10^6

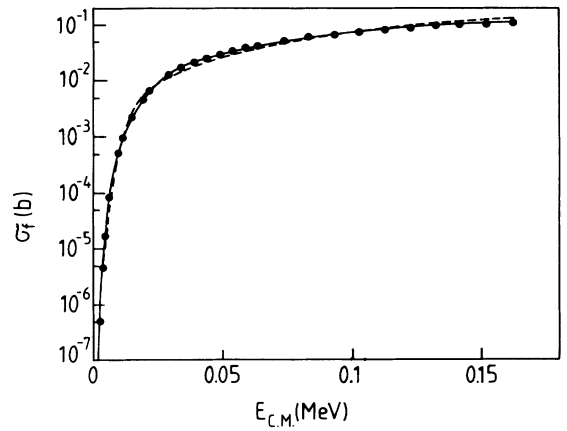

FIG. 3. Same as Fig. 2 for the reactions $^2H(d,p)^3H$, $^2H(d,n)^3He$ [15].

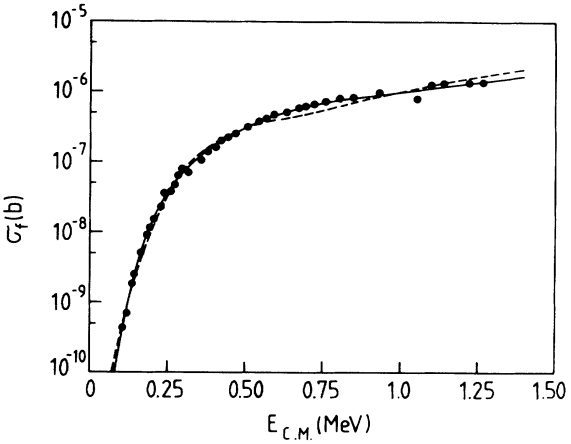

FIG. 6. Same as Fig. 2 for the reaction $^3He(\alpha,\gamma)^7Be$ [18].

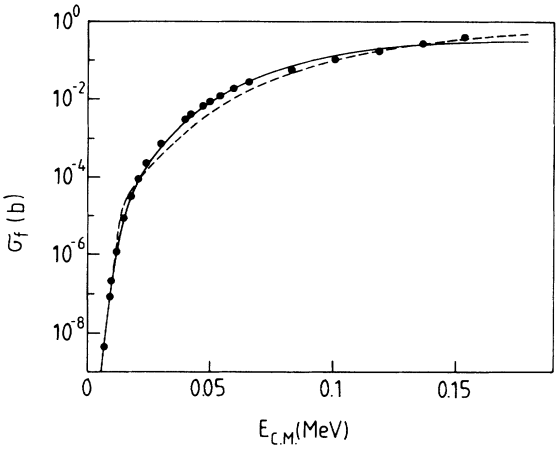

FIG. 4. Same as Fig. 2 for the reaction $^3He(d,p)^4He$ [15].

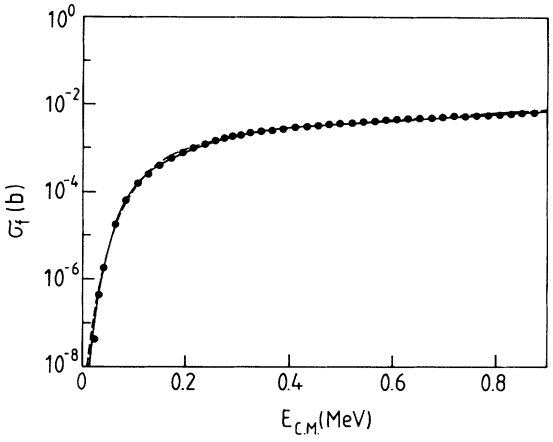

FIG. 7. Same as Fig. 2 for the reaction $^7Li(p,\alpha)^4He$ [19].

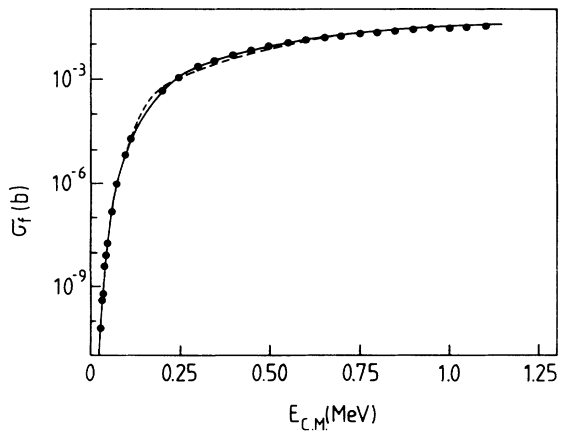

FIG. 5. Same as Fig. 2 for the reaction $^3He(^3He,2p)^4He$ [16,17].

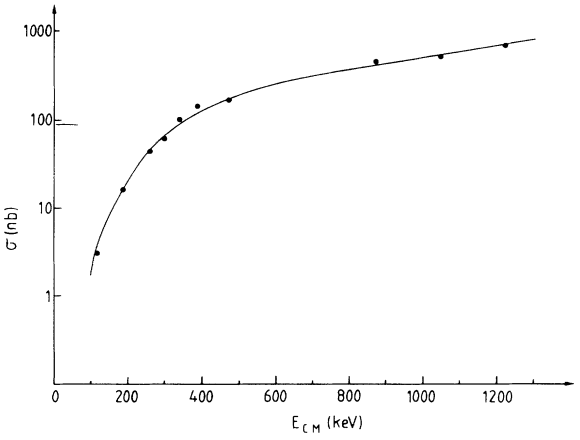

FIG. 8. Same as Fig. 2 for the reaction $^7Be(p,\gamma)^8B$ [20].

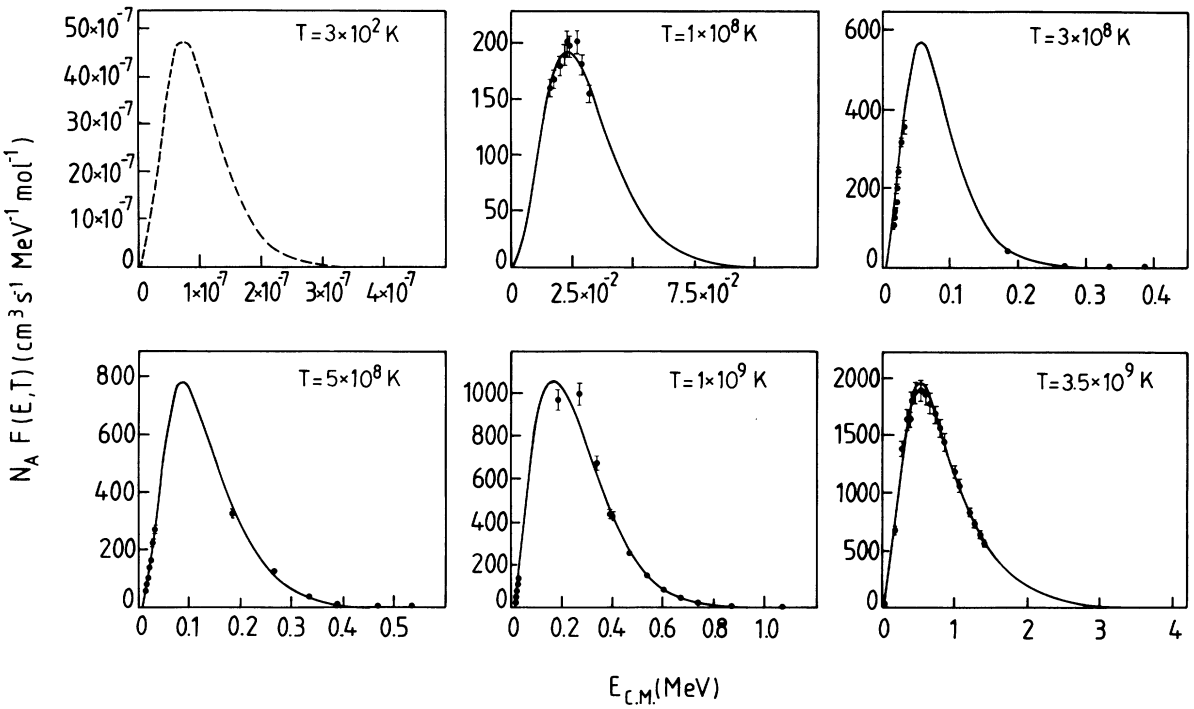

FIG. 9. Comparison at different temperatures between the integrand of Eq. (11) obtained by using for $\sigma(E)$ the experimental values and the integrand of Eq. (16) (solid lines) for the reaction $^2H(p,\gamma)^3He$ [12,14]. Both integrands are multiplied by Avogadro's number N_A. The dashed line represents an extrapolation at low temperature.

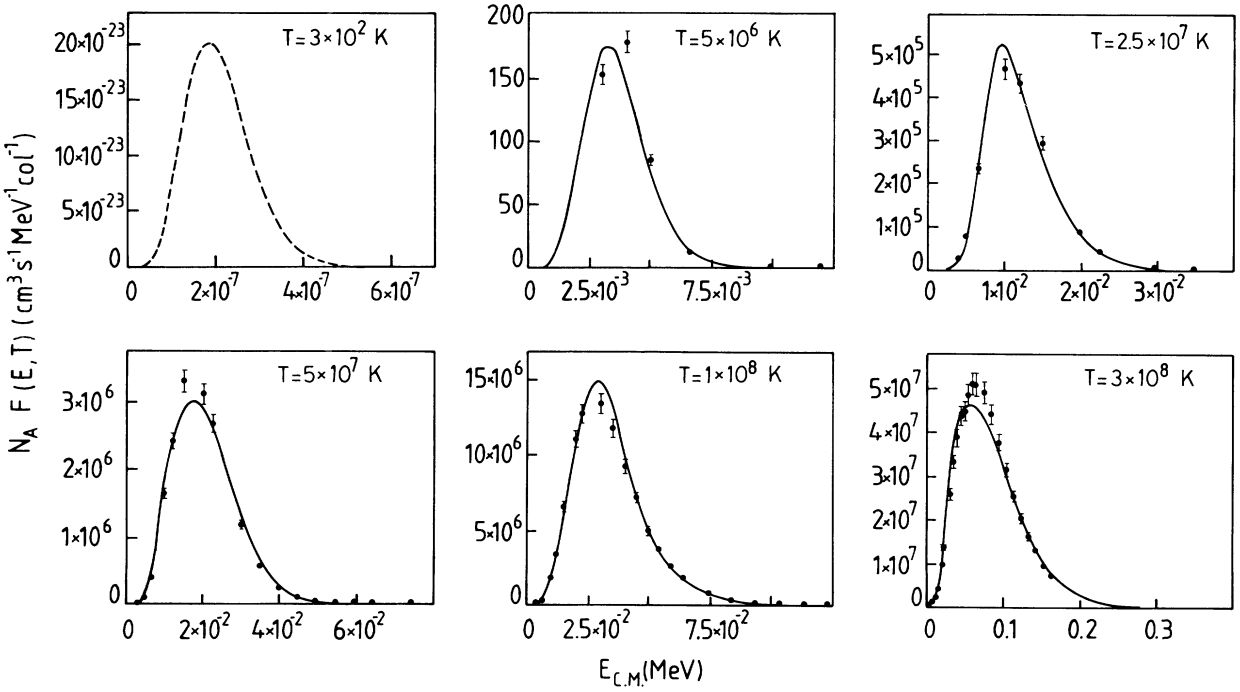

FIG. 10. Same as Fig. 9 for the reactions $^2H(d,p)^3H$, $^2H(d,n)^3He$ [15].

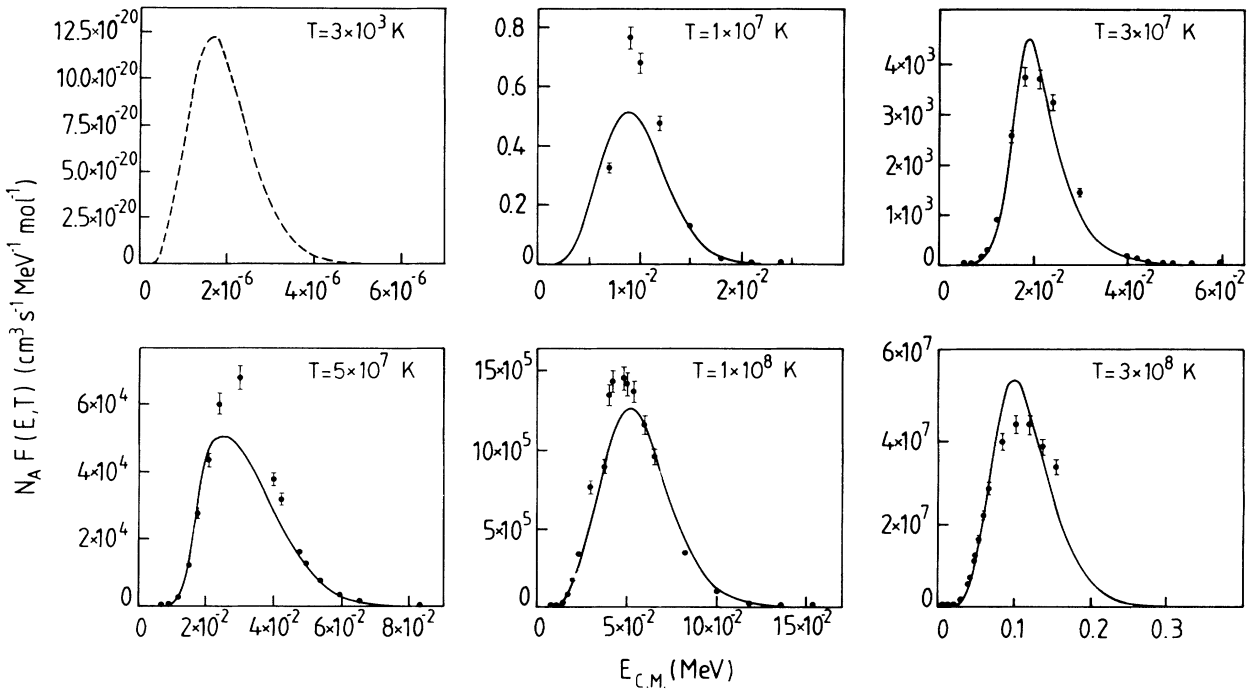

FIG. 11. Same as Fig. 9 for the reaction ^{3}He$(d,p)^4$He [15].

ly considered [1–7]. Moreover, the reaction ^{7}Be$(p,\gamma)^8$B is investigated by using these procedures.

II. SHADOW MODEL

In the shadow model, the fusion cross section is obtained by assuming that the fusion process is the shadow of the elastic scattering [8,9]. From this assumption it follows that the fusion cross section can be written

$$\bar{\sigma}_f = 2\pi \int_{\vartheta_f}^{\pi} \sigma_R(\vartheta)\sin(\vartheta)d\vartheta = \pi(\eta/k)^2 \mathrm{cotan}^2(\vartheta_f/2) = \pi b_f^2 , \quad (1)$$

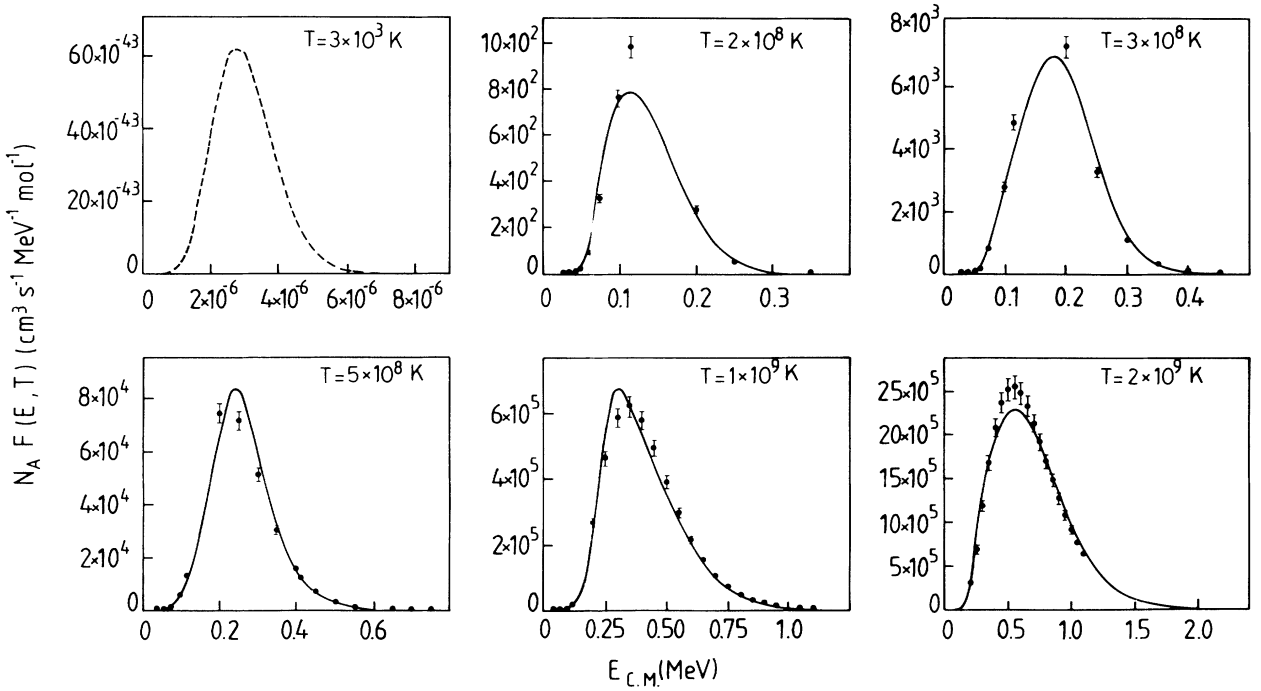

FIG. 12. Same as Fig. 9 for the reaction ^{3}He$(^3$He$,2p)^4$He [16,17].

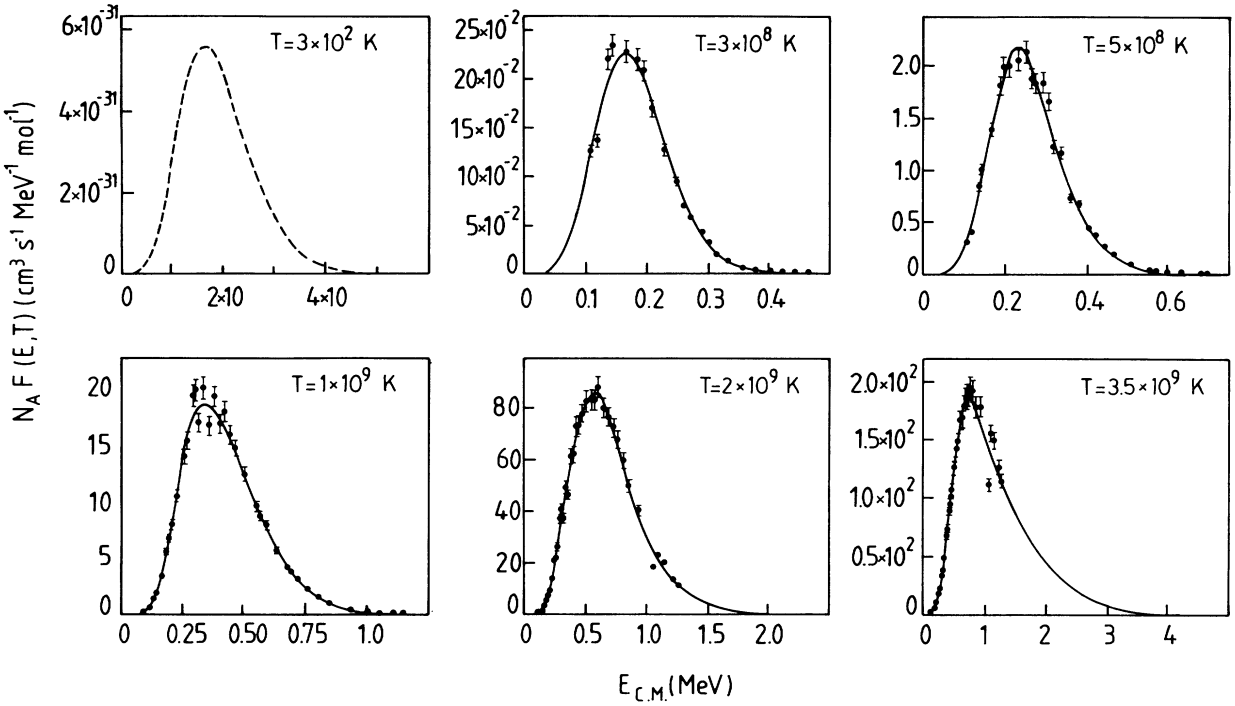

FIG. 13. Same as Fig. 9 for the reaction ^{3}He$(\alpha,\gamma)^7$Be [18].

where $\sigma_R(\vartheta)$ is the Rutherford cross section, η is the Coulomb parameter, k is the wave number, $[\vartheta_f-\pi]$ is the shadow region (see Fig. 1), and b_f is the impact parameter corresponding to ϑ_f.

We remind the reader than in Rutherford scattering the scattering angle is

$$\vartheta_f = 2\arcsin\left[\frac{Z_1Z_2e^2}{2ER_f - Z_1Z_2e^2}\right], \tag{2}$$

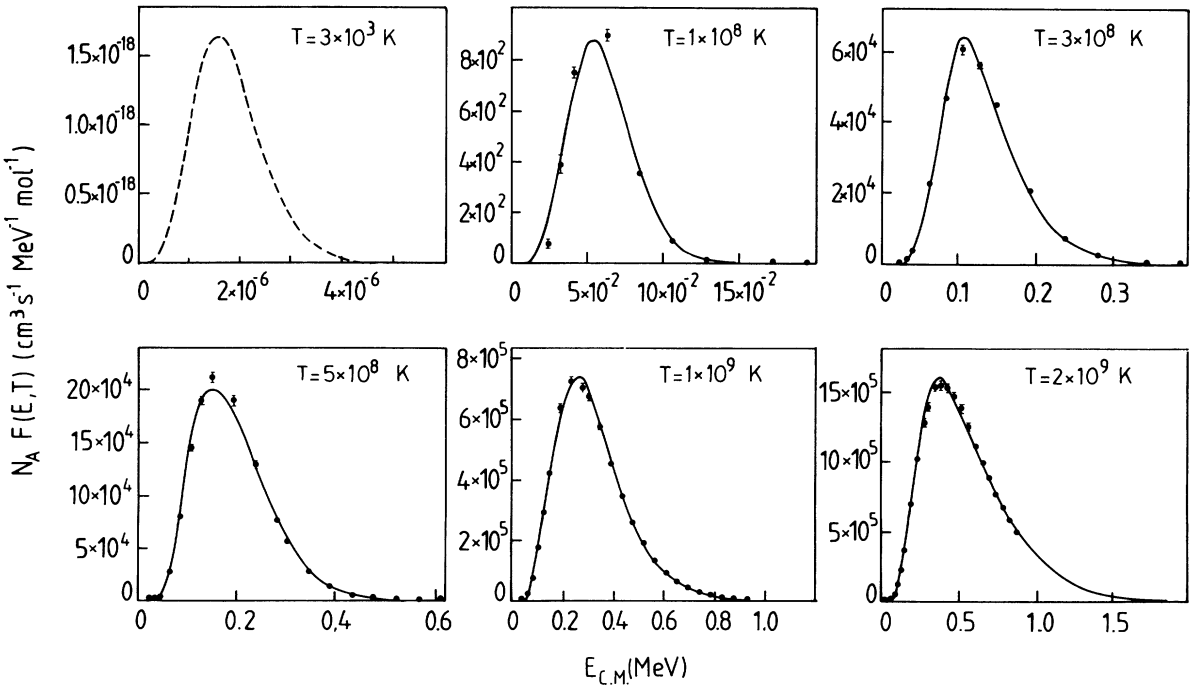

FIG. 14. Same as Fig. 9 for the reaction ^{7}Li$(p,\alpha)^4$He [19].

where E is the center-of-mass energy and R_f is the distance of closest approach of the trajectory with impact parameter b_f. By using Eq. (2), Eq. (1) can be rewritten as

$$\bar{\sigma}_f = \pi R_f^2 (1 - 2\eta/kR_f) . \quad (3)$$

In Ref. [9] we showed that the critical value of the distance of closest approach, R_f, can be written as

$$R_f = (2\eta/k)(1 + \exp\{-\exp[\exp(y)]\}) , \quad (4)$$

where

$$y = (E_B - E)/E_S \quad (5)$$

and E_B and E_S are two parameters to be determined.

By using Eqs. (4) and (5), Eq. (3) can be rewritten as

$$\bar{\sigma}_f = \pi(2\eta/k)^2[1 + G(y)]G(y) , \quad (6)$$

where

$$G(y) = \exp\{-\exp[\exp(y)]\} . \quad (7)$$

The parameters E_B, E_S can be determined by comparing the values of fusion cross section σ_f obtained by using Eq. (6) with the experimental data. We remind the reader than E_B is the energy of the Coulomb barrier and E_S is a scale parameter [9]. At very low energy, we suggest to modify Eq. (6) as follows [4–7]:

$$\sigma_f = \bar{\sigma}_f [1 - g(y)][1 - g_1(y)] , \quad (8)$$

where

$$g(y) = \exp\left[-\left[\frac{d-y}{d-y_m} \right]^{\gamma_1} 2.789 \right] ,$$

$$g_1(y) = \exp\left[-\left[\frac{d-y}{d-y_1} \right]^{\gamma_2} 2.789 \right] , \quad (9)$$

$$d = E_B/E_S, \quad y_m = (E_B - E_m)/E_S, \quad y_1 = (E_B - E_1)/E_S ,$$

and E_B, E_S, E_m, E_1, γ_1, and γ_2 are parameters to be determined.

A crucial point of our approach is the determination of these parameters. In Ref. [6] we suggested to assume for E_m the value of the energy at which $\bar{\sigma}_f(E)$ attains a minimum value and for E_1 the value of the energy at which $\ln(\bar{\sigma}_f)$ shows an inflection point, so that E_B, E_S, γ_1, and γ_2 can be determined by comparing the values of σ_f defined in Eq. (8), with the experimental values of the fusion cross section.

The theoretical values of σ_f can be determined, also, by considering E_B, E_S, y_m, y_1, γ_1, and γ_2 free parameters. A comparison between the experimental values of fusion cross sections and the values of σ_f obtained by using four or six free parameters is showed in Figs. 2–8. In Table I the values of these two sets of parameters are reported.

III. NUCLEAR REACTION RATES

The study of stellar evolution requires the knowledge of the reaction rate. In the usual astrophysical environments, the interacting nuclei collide with a Maxwell-Boltzmann distribution of relative velocity, and the reaction rate is given by

$$r_{12} = n_1 n_2 \langle \sigma v \rangle / (1 + \delta_{12}) , \quad (10)$$

with

$$\langle \sigma v \rangle = \int_0^\infty [(8/\pi) M_{12} (kT)^3]^{1/2} \sigma(E) \times \exp(-E/kT) E \, dE , \quad (11)$$

where M_{12} is the reduced mass of particles 1 and 2, n_1 and n_2 are the number densities of particles 1 and 2, v is the relative velocity, E is the center-of-mass energy, k is Boltzmann's constant, and T is the temperature. For nonresonant reactions the cross section is usually written as [10]

$$\sigma(E) = [S(E)/E] \exp(-2\pi\eta) , \quad (12)$$

with

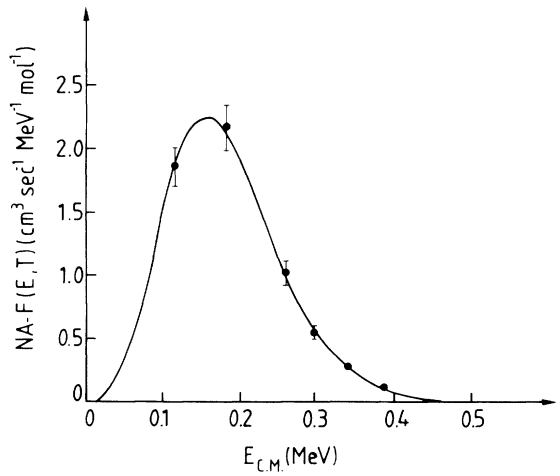

FIG. 15. Same as Fig. 9 for the reaction ^{7}Be$(p,\gamma)^8$B at $T = 4.0 \times 10^8$ K [20].

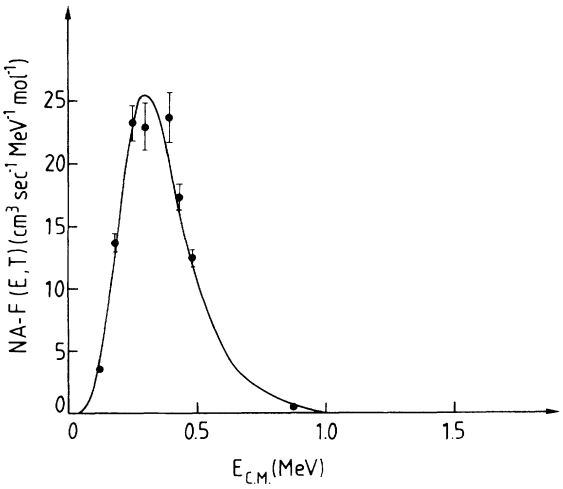

FIG. 16. Same as Fig. 9 for the reaction ^{7}Be$(p,\gamma)^8$B at $T = -1.0 \times 10^9$ K [20].

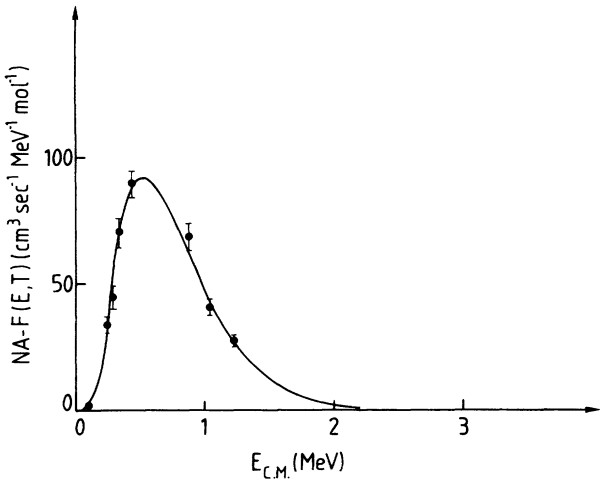

FIG. 17. Same as Fig. 9 for the reaction $^{7}Be(p,\gamma)^{8}B$ at $T=2.5\times10^{9}$ K [20].

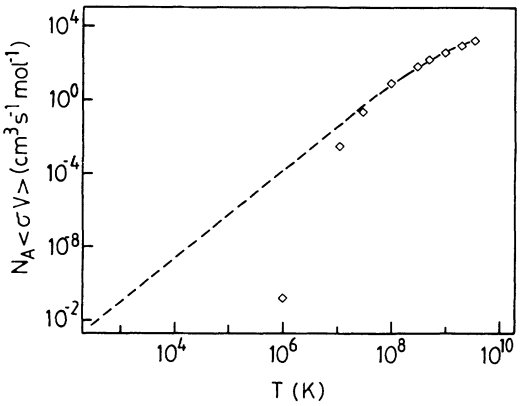

FIG. 18. Comparison between the values of $N_A\langle\sigma v\rangle$ reported in Ref. [11] and the results of our approach (solid line) for the system $^{2}H(p,\gamma)^{3}He$ [12–14]. The dashed line represents the extrapolated values obtained by our method in the range where there are not experimental data.

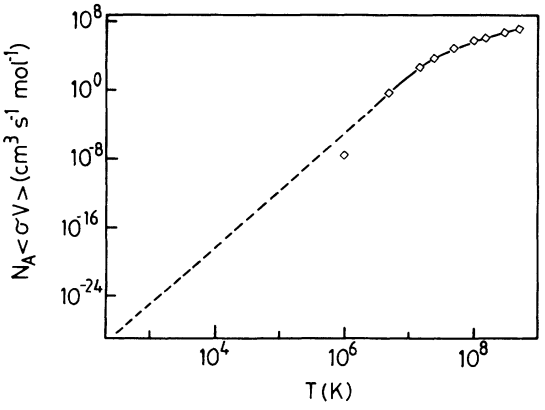

FIG. 19. Same as Fig. 18 for the reactions $^{2}H(d,p)^{3}H$, $^{2}H(d,n)^{3}He$ [15].

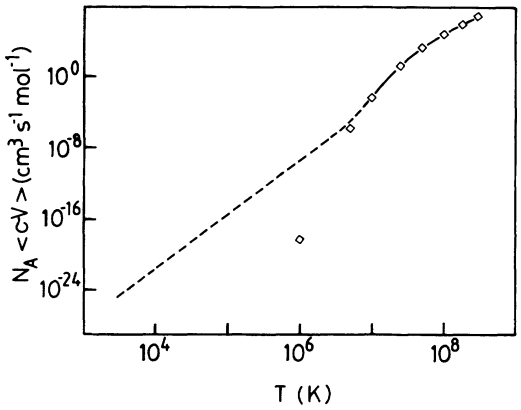

FIG. 20. Same as Fig. 18 for the reaction $^{3}He(d,p)^{4}He$ [15].

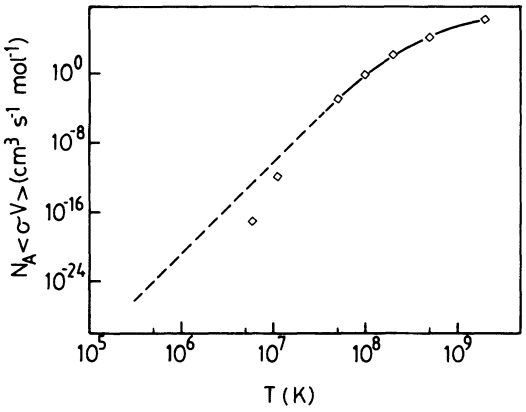

FIG. 21. Same as Fig. 18 for the reaction $^{3}He(^{3}He,2p)^{4}He$ [16,17].

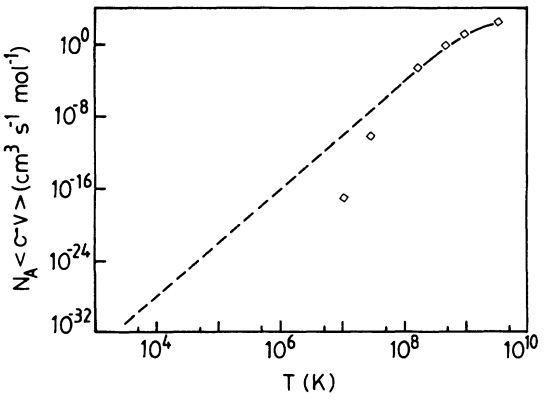

FIG. 22. Same as Fig. 18 for the reaction $^{3}He(\alpha,\gamma)^{7}Be$ [18].

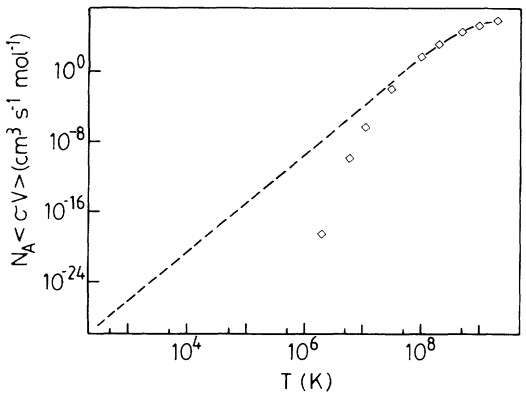

FIG. 23. Same as Fig. 18 for the reaction ^{7}Li$(p,\alpha)^4$He [19].

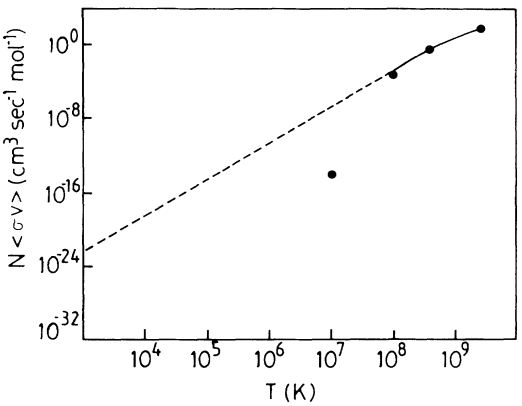

FIG. 24. Same as Fig. 18 for the reaction ^{7}Be$(p,\gamma)^8$B [20].

$$2\pi\eta = 2\pi\left[\frac{Z_1 Z_2 e^2}{\hbar v}\right] = (E_G/E)^{1/2} . \quad (13)$$

E_G is the Gamow energy, η is the Coulomb parameter, Z_1 and Z_2 are integral nuclear charges of the two particles, and $S(E)$ is the nuclear astrophysical S factor. By using Eqs. (12) and (13), Eq. (11) becomes

$$\langle\sigma v\rangle = \int_0^\infty [(8/\pi)M_{12}(kT)^3]^{1/2} S(E) \times \exp[-(E/kT)-(E_G/E)^{1/2}]dE . \quad (14)$$

The energy dependence of the integral is determined predominantly by the product of the Maxwell Boltzmann factor and the penetration factor, leading to a peak of the integrand with its maximum at an energy $E_{\max}$:

$$E_{\max} = \left[\pi e^2 Z_1 Z_2 kT(M_{12}c^2/2)^{1/2}\hbar c^2\right]^{2/3} . \quad (15)$$

By using for the cross section σ_f the expression given by the shadow model [see Eqs. (8) and (9)], the cross-section factor can be rewritten as

$$\langle\sigma v\rangle = \int_0^\infty [(8/\pi)M_{12}(kT)^3]^{1/2}\sigma_f(E) \times \exp(-E/kT)E\,dE = \int_0^\infty F(E,T)dE . \quad (16)$$

The integrand of Eq. (16) versus the energy shows a peak so that in Refs. [2–5] we suggested as approximate method to determine the cross-section factor for light systems. In the present paper, the cross-section factor $\langle\sigma v\rangle$ is obtained by using a numerical integration with a suitable computer program. A comparison between the integrand of Eq. (11) obtained by using for $\sigma_f(E)$ the experimental values of the fusion cross section and the integrand of Eq. (16) is shown in Figs. 9–17 for different systems and at different temperatures. The dashed line represents an extrapolation at very low temperature. The integrand functions have been obtained by using a six free parameters fit for σ_f.

In Figs. 18–24 the values of $N_A\langle\sigma v\rangle$ (N_A is Avogadro's number) reported in Ref. [11] (romboids or solid circles) are compared with the results obtained by using the shadow model (solid line). The dashed line represents the extrapolation obtained by our method in the range where there are not experimental results. The same comparison is also shown in Table II.

Finally, we can assert that if the shadow model is able to describe the fusion process also at very low energies, where there are not experimental results, then, for any temperature, the cross-section factor can be obtained by using our approach.

IV. CONCLUSIONS

From our analysis it follows that by extrapolating the values of the reaction rates at energies where there are not experimental results we obtain values which are different from those present in the literature and obtained by using the "Gamow formula" for the fusion cross section. Our approach, based on a phenomenological analysis of many fusion reactions, suggests a new understanding of the fusion process; moreover, astrophysical implications of the new values of the reaction rates could be investigated and the neutrino fluxes could be determined by using in the stellar evolutionary codes the new values of the reaction rates.

[1] A. Scalia, J. Ital. Astron. Soc. **60**, 99 (1989).
[2] A. Scalia, Nuovo Cimento A **100**, 559 (1988); **101**, 355 (1989).
[3] A. Scalia, Nuovo Cimento A **101**, 795 (1989).
[4] A. Scalia, Nuovo Cimento A **102**, 953 (1989); **102**, 1101 (1989); **102**, 1105 (1989).
[5] A. Scalia, Nuovo Cimento A **103**, 47 (1990); **103**, 85 (1990); **103**, 213 (1990); **103**, 255 (1990); **103**, 927 (1990); **103**, 1177 (1990).
[6] R. Giordano, P. Figuera, S. Pirrone, and A. Scalia, Nuovo Cimento A **103**, 415 (1990).
[7] A. Scalia, Nuovo Cimento A **104** 563 (1991).
[8] A. Scalia, Nuovo Cimento A **104**, 1467 (1991).
[9] A. Scalia, Nuovo Cimento A **105**, 233 (1992).
[10] D. D. Clayton, *Principles of Stellar Evolution and Nucleosynthesis* (McGraw-Hill, New York, 1968).
[11] G. R. Caughlan, W. A. Fowler, M. J. Harris, and B. A. Zimmerman, At. Data Nucl. Data Tables **32**, 197 (1985).

[12] G. M. Griffits and J. B. Warren, Proc. Phys. Soc. (London) A **68**, 781 (1955).
[13] G. M. Griffits, E. A. Larson, and L. P. Robertson, Can. J. Phys. **40**, 402 (1962).
[14] G. M. Griffits, M. Lal, and C. D. Scarfe, Can. J. Phys. **41**, 724 (1963).
[15] A. Krauss, H. W. Becker, H. P. Trautvettey, C. Rolfs, and K. Brand, Nucl. Phys. **A465**, 150 (1987).
[16] M. R. Dwarakanath and H. Winkler, Phys. Rev. C **4**, 1532 (1971).
[17] M. R. Dwarakanath, Phys. Rev. C **9**, 805 (1974).
[18] H. Krawinkel, H. W. Becker, L. Buchmann, J. Gorres, K. U. Kettner, W. E. Kieser, R. Santo, P. Schmalbrok, H. P. Trautvetter, A. Vlieks, C. Rolfs, J. W. Hammer, R. E. Azuma, and W. S. Rodney, Z. Phys. A **304**, 307 (1982).
[19] C. Rolfs and R. W. Kavanagh, Nucl. Phys. **A455**, 179 (1986).
[20] B. W. Filippone, A. J. Elwyn, C. N. Davids, and D. D. Koetke, Phys. Rev. C **28**, 2222 (1983).